

Detection of Transition by Infrared Image Techniques

Armin Quast
DFVLR
Braunschweig, Germany

Presented at the XX OSTIV Congress, Benalla, Australia (1987)

Introduction

Transition lines where laminar flow changes to turbulent flow are usually detected by the well-known oil-flow method or sublimation techniques (acenaphthene). Both these methods have the disadvantage that the flow may be affected by the visualization material. Besides this, these methods are rather time consuming and, therefore, depending on tunnel size, also costly. Other methods like microphone, hot wire and hot film can give only a point by point information whether the boundary layer is laminar or turbulent. Therefore, the use of these methods is also time consuming or very large and costly equipment is required.

Reynolds analogy between skin friction and heat transfer

According to Reynolds analogy heat transfer coefficient α_h depends in a simplified form from the following parameters:

$$\alpha_h = \frac{1}{2} c'_f \frac{U \cdot \lambda}{\nu}$$

where c'_f is the skin friction coefficient, U the local velocity, λ the heat conductivity of the fluid and ν the kinematic viscosity. It should be noted that λ , as far as aircraft are concerned, does not change with pressure. The formula explains the well-known fact, that heat transfer in laminar boundary layer is small because skin friction is small and that heat transfer in turbulent boundary layer is much higher because skin friction is higher.

Figure 1 shows the skin friction coefficient of a flat plate as a function of local Reynolds number Re , for three different transition Reynolds numbers $Re_{x,TR}$. Transition Reynolds number depends on flow quality, $Re_{x,TR} = 5.106$ is of the order of free flight conditions. We see that at the transition point, skin friction jumps by more than a factor of 10. According to Reynolds analogy also heat transfer changes by the same factor.

If there is a temperature difference between the fluid and the airfoil model surface, the latter will adopt different temperatures whether flow is laminar or turbulent. As in turbulent flow, and especially just behind transition, heat transfer is high, the model will adopt nearly the temperature of the fluid. On the other hand, the model temperature will remain nearly unchanged in the laminar boundary layer just upstream of the transition location, where the wall shear stress is minimum.

Infrared image system

Modern nitrogen cooled infrared scanner systems are able to resolve radiation temperature differences down to $0,1^\circ\text{C}$. Good pictures are obtained with temperature differences of 1°C and excellent pictures with 2°C . As shown in Figure 1, the skin friction changes with transition by approximately a factor of ten. Therefore, on an infrared picture, the transition line is marked by a sharp step in surface temperature which becomes visible on the screen in a change from dark to white. A representation of infrared information by colour-step picture for the detection of the transition location (instead of gray steps as in all figures of this paper) proved to be not so useful.

The origin of temperature differences

Observations showed, that in many wind tunnels the temperature differences necessary for infrared pictures are present without any internal or external heating of the model surface. This is normally due to the radiation exchange between the model and the walls of the closed test section or the walls of the measuring hall in the case of an open test section. In other cases the temperature differences for a good picture, were obtained by switching on and off wind tunnel cooling. This method is only effective, if the model surface and the test section surface do not have the same heat capacity (better temperature propagation coefficient).

Also, free flight tests were done, utilizing radiation into space or sun radiation. External heating by radiators is not recommended because of reflections into the infrared system. Nevertheless, the most comfortable arrangement is that of an internally heated model. The analogy between measurements with hot films and with an infrared system is quite obvious.

With the exception of the sun radiation the colour paint of the model has no influence on the infrared picture. Normally, models were covered with ground and polished white painting like sailplanes. Strips of red or dark colour are not visible on the infrared image. Markings were done with aluminum strips which naturally have the same temperature as the model surface at their location. But brightening metallic surfaces gave a considerably lower radiation coefficient resulting in less radiation, which the infrared system interprets as a lower temperature.

Models were manufactured of fiber reinforced plastic, to reduce or avoid temperature flattening by a high thermal conductivity in the direction of the model surface.

Examples of transition detection by infrared technique

Figure 2 shows an infrared picture of an ASW-22 HQ17/14.38 airfoil upper side, the model being colder than the air. Airflow is from left to right as in all other figures of this paper. The gray colour is darkening from the leading edge to about 70%, corresponding to a decreasing skin friction of the laminar flow with increasing airfoil chord. Since the model is colder than air, pure white correlates with high temperature and high skin friction whereas dark indicates lower temperature and low friction. Downstream of the transition line the skin friction of the fresh turbulent boundary layer is very high, resulting in a white colour. Downstream of the transition, the skin friction of a turbulent boundary layer diminishes, resulting in a certain darkening. At the bottom of Figure 2, the well known turbulent wedges originating from aluminum strips are visible. These wedges are characteristic for laminar flow and do not occur in turbulent flow. Note that the colour in the wedge downstream of the transition location is gray, in contrast to the part of the model without wedges at the same chord position. This indicates lower skin friction due to a thicker turbulent boundary layer downstream of the wedges compared to the skin friction in undisturbed flow.

On the upper part of Figure 2, a small forward shift of transition location is visible. This is due to the presence of a line of pressure holes which were one behind another. This is a nice demonstration of sub-critical disturbances in a laminar boundary layer which do not result in a turbulent wedge. Nevertheless, the pressure holes do influence the laminar boundary in that way that the transition point moves upstream.

Figure 3 demonstrates the development of the transition line with increasing angle of attack. At $\alpha = 10^\circ$ the laminar flow in the undisturbed part is up to 65 % of the chord. At $\alpha = 15^\circ$ the laminar flow is reduced to about 22% of the chord. As known from pressure distribution and drag measurements at $\alpha = 15^\circ$ a turbulent separation develops from the trailing edge. This turbulent separation can not be identified by infrared technique. Apparently net heat transfer does not change sufficiently, whether the turbulent layer is separated or not.

Figure 4 shows a laminar separation bubble, which also was visible in Figures 2 and 3. Whereas, on an infrared picture the transition is clearly visible, the separation point is hard to detect. The apparent separation point depends on the brightness setting of the monitor and, therefore, problems arise with the reproductivity. Indeed, just upstream of the separation, the skin friction is zero, and in a laminar separation bubble, the skin friction is zero to, or very small.

Figure 5 demonstrates a direct laminar-turbulent transition at higher Reynolds numbers¹, which at $\alpha = -1,5^\circ$ angle of attack is merely a straight line. At $\alpha = -1^\circ$ a very scattered line is visible, although the model was very accurate. This demonstrates the danger of misleading results of point by point

¹ or at certain types of pressure distribution at lower Reynolds numbers

measurements of the transition location by other methods.

Figure 6 shows an oil-flow picture and an infrared picture of the same wing at identical flow conditions. The aluminum strip was removed for the oil-flow picture. Note that the lens system of the infrared camera apparently distorts the picture in a barrel-like way.

The oil-flow picture indicates a laminar separation bubble beginning at $x/c = 0,58$ and a transition location at $x/c = 0,65$. The same values can be derived from the infrared image. In this case the oil has no detectable influence on the development of the laminar boundary layer and on the transition location. A forward shift of the transition location by the row of pressure holes cannot be detected in the oil-flow picture, because of the contamination of the orifices by the oil. As described in the discussion of Figure 4, a laminar separation can hardly be detected on an infrared image.

One difference between the methods lies in the time for producing a picture. Oil flow pictures take at least 10-15 minutes to be processed, whereas for an infrared picture only, the normal time for pressure reading (1 min.) is necessary.

The picture on the infrared systems monitor can be switched from the normal mode to an inverted mode, as demonstrated in Figure 7. The reading of the transition locations from both modes differ from 50% in normal mode to 51 % in the inverted mode. Such a difference is within the normal experimental error.

The effect of strips at different chordwise positions is shown in Figure 8. The strips are all of the same height, which is subcritical. A strip at $x/c = 0,65$ does not have any effect on the transition location whereas the strip at $x/c = 0,25$ gives a small forward shift of the transition location. A remarkable shift is due to the strip at $x/c = 0,15$. At this position, the laminar boundary layer seems to be very sensitive.

An infrared image from a wing taken in flight out of the cabin of a small airplane is shown in Figure 9. The wing of the airplane was equipped with a glove for laminar flow investigations. The glove was painted red in order to enlarge the influence of sun radiation and to enable the application of the acenaphthene technique. Transition is clearly visible, in this case in the inverted mode.

Importance of infrared systems

Although the price of an infrared system lies in the order of \$50,000 US the investment is easily counterbalanced by the fact that transition measurements can be done in a shorter time and, therefore, wind tunnel time is saved.

By this method, transition is not only detected point by point, but a certain area of a wing can be investigated. Thus, an average transition position can be established. Furthermore, the model can be observed systematically to detect contaminations by insects in free flight and dust, plasticine and other particles in wind tunnels. This application of the infrared technique will avoid misleading measurements.

Conclusions

The infrared technique is a powerful tool for transition line detection. The whole model area can be under surveillance with respect to turbulent wedges, or even smaller sub-critical disturbances in the laminar boundary layer. This technique has been successfully applied in different wind tunnels and in free flight experiments. In most cases "natural" temperature differences between the model and the fluid gave reasonable or good infrared images. In one case, switching on and off the wind tunnel cooling systems gave good results. Nevertheless, the most comfortable means is the internally heated model. Infrared technique is also suitable for free flight experiments.

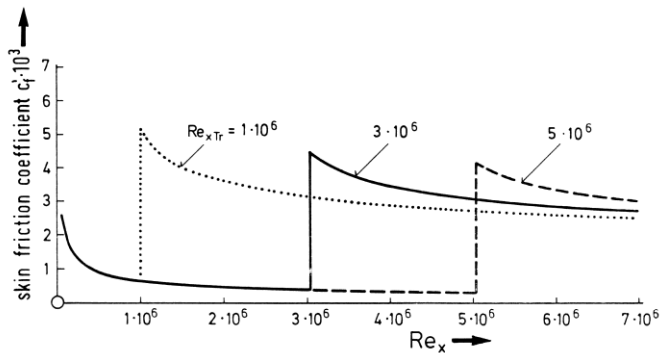


Figure 1 Skin friction coefficient $c'f$ of flat plate versus local Reynolds number Re_x as function of Transition Reynolds number Re_{xTr} .

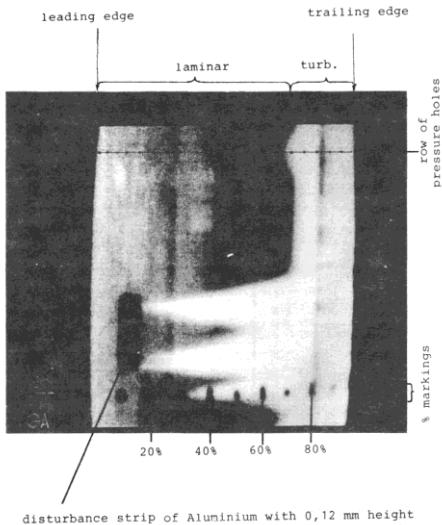


Figure 2 Characteristics of an infrared image.

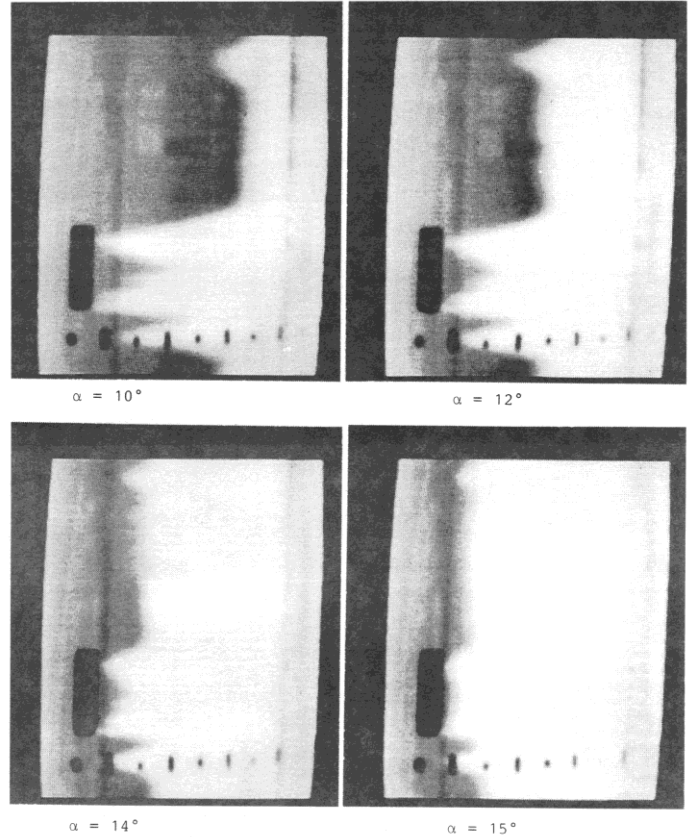


Figure 3 Position of transition line with increasing angle of attack HQ17/14.38; upper side; $\alpha_k = 8^\circ$, $Re = 1,5 \cdot 10^6$; meas. MUB

laminar separation bubble

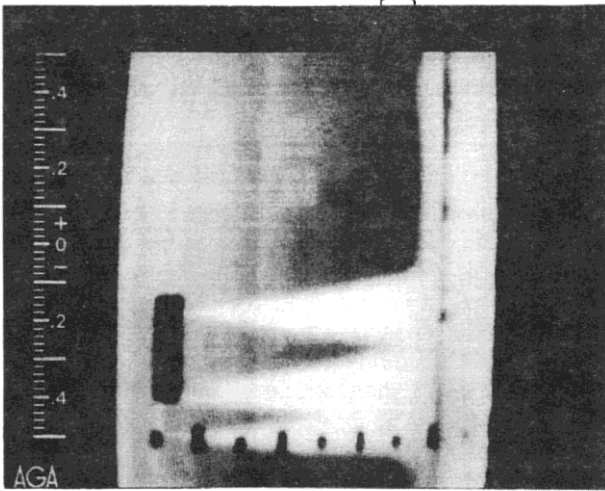


Figure 4 Appearance of laminar separation bubble on an infrared image.

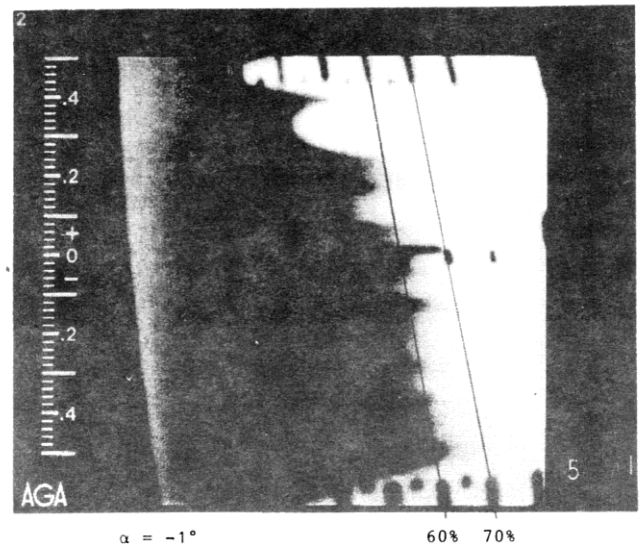
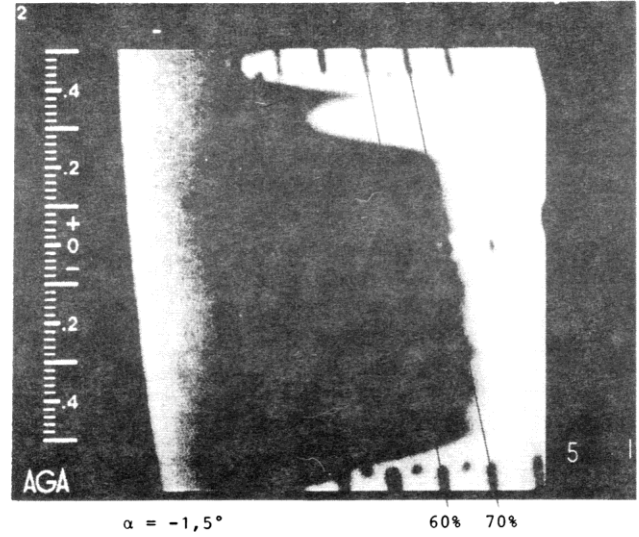
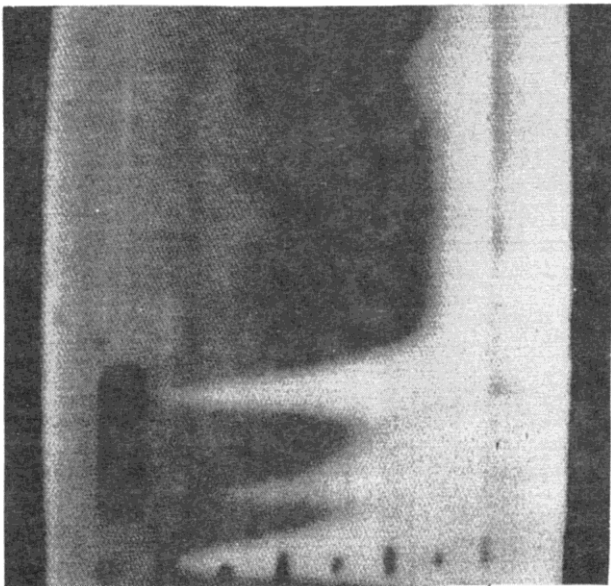
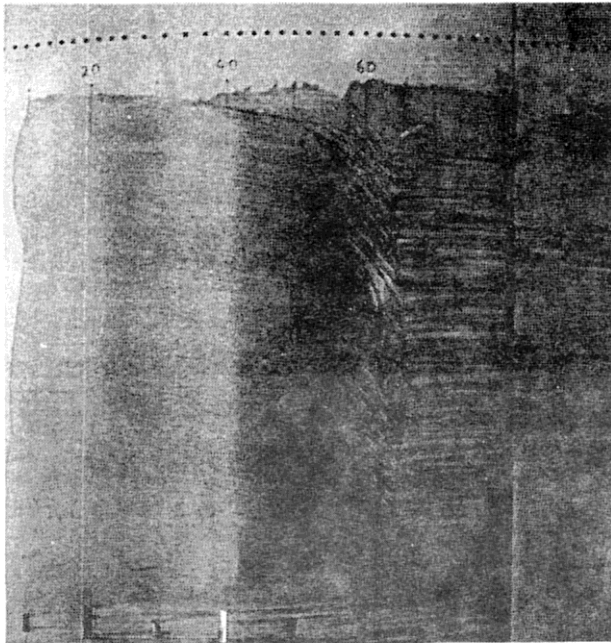


Figure 5 Different transition front locations at different angles of attack.



20% 40% 60% 80%

Figure 6 Comparison between oil flow picture and infrared image; HQ17/14.38; $\alpha = 8^\circ$; $\alpha k = 0^\circ$, $Re = 1,5 \cdot 10^6$; meas. MUB

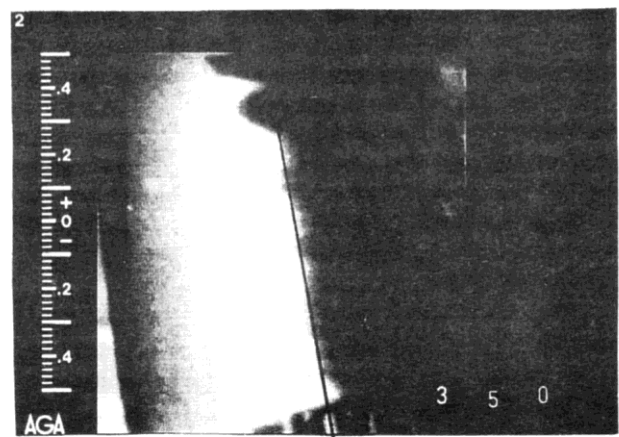
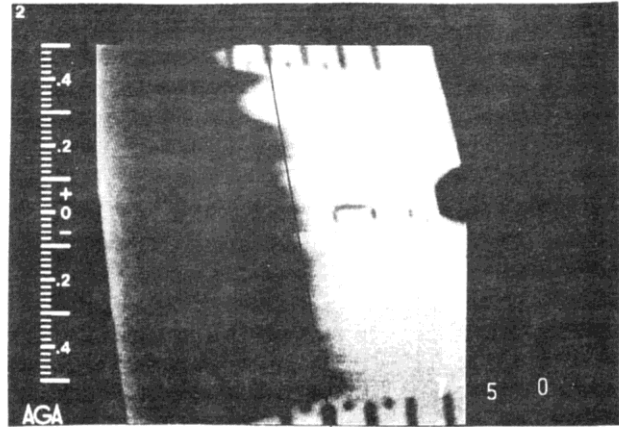


Figure 7 Normal (upper figure) and inverted (lower figure) infrared image.

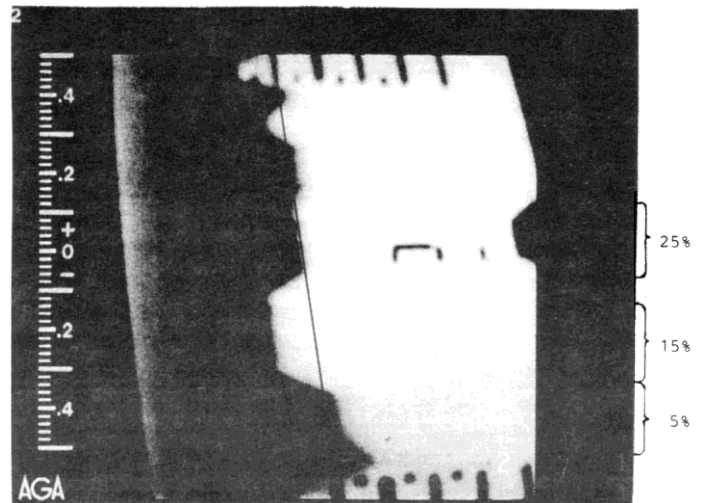


Figure 8 Effect of different disturbance positions on transition. LFU glove; $\alpha = 0,25^\circ$; $\alpha k = 0^\circ$; $Re = 9,5 \cdot 10^6$; disturbance height 0,055 mm; measurement DNW

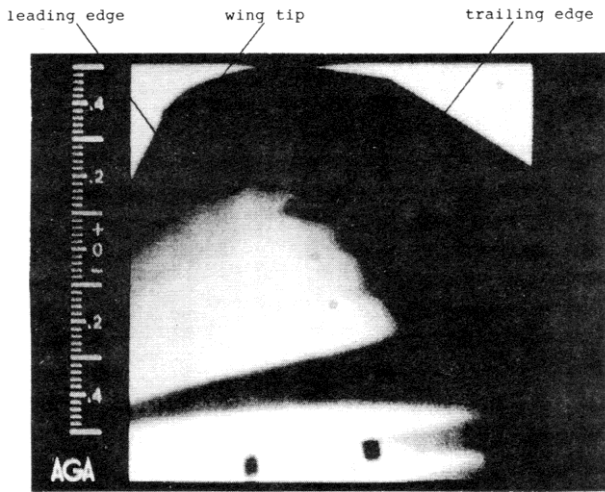
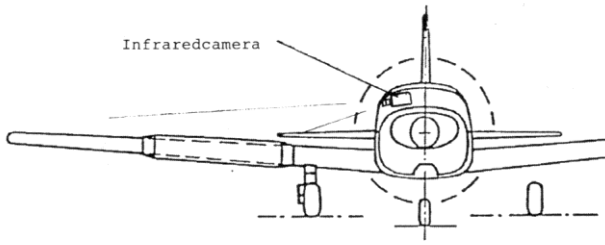


Figure 9 Infrared image of a motorcraft glove in free flight, inverted image; laminar boundary layer white, turbulent dark.